Baseload Solar Power for California?

Ammonia-based Solar Energy Storage Using Trough Concentrators – A Study of Heat Losses

R. Dunn, K. Lovegrove, G. Burgess
Centre for Sustainable Energy Systems
Department of Engineering
Australian National University
ACT 0200
AUSTRALIA
E-mail: u3963648@anu.edu.au, Keith.Lovegrove@anu.edu.au, Greg.Burgess@anu.edu.au

Heat losses from a trough cavity receiver were investigated in order to eventually optimise the reactor geometry for ammonia-based solar energy storage with troughs, which are prominent in the SEGs plants of California. To this end, experiments were performed with a small-scale receiver containing heating elements. This gave free convection loss coefficient values from 0.3 to 11.8 W/(m^2.^{o}C) from 90 degrees inclination to zero degrees inclination respectively. This accounted for 2 to 40% of the total heat losses in each case. An attempt to apply the free convection correlation developed by Paitoonsurikarn (2006) showed that in its current form, the correlation does not accurately predict these free convection losses. Application of the heat loss model to actual solar dissociation results showed that an iterative heat loss calculation is necessary to accurately represent the heat loss at the reactor, and that further investigation of forced convection losses is necessary.

1. INTRODUCTION

1.1. Storing Solar Energy with Ammonia

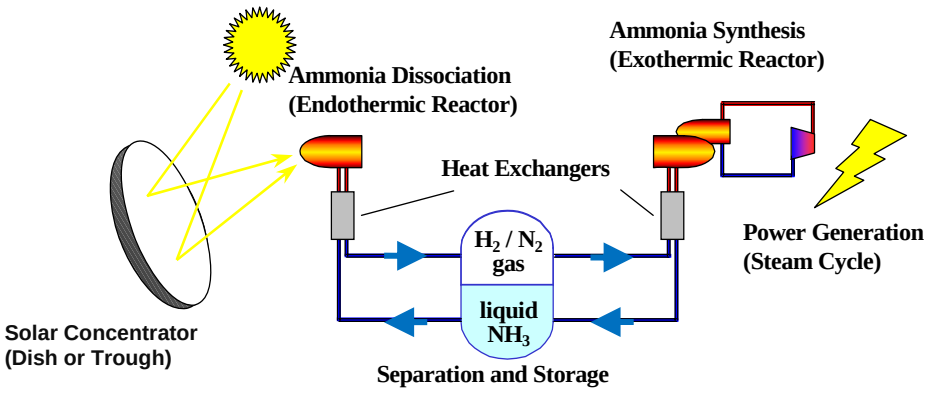

Figure 1—1 : An overview of ammonia-based solar energy storage. (Sourced from Lovegrove *et al.* (2004a).)

For several years, the *ANU Solar Thermal Research Group* has investigated solar energy storage, using ammonia as a storage medium. This involves using a parabolic mirror to concentrate solar radiation, which provides the heat (ΔH) to dissociate ammonia (NH_3) during the day, according to Equation (1). The resulting nitrogen and hydrogen gases (N_2 and H_2) are stored to later be re-synthesised into ammonia at night or on a cloudy day. This reaction releases heat which creates steam used to generate electricity. This entire process can be summarised according to the reversible

reaction in Equation (1). The reaction proceeds from left to right during the day, and from right to left when electricity generation is desired. Thus electricity sourced from the sun can be produced on demand.

$$NH_3 + \Delta H \xleftrightarrow{\text{RuC catalyst}} \tfrac{1}{2}N_2 + \tfrac{3}{2}H_2 \quad \textbf{(1)}$$

1.2. Project Outline

Previous work has mainly centred on optimising the storage process for parabolic dish concentrators. However, parabolic trough concentrators constitute a large existing market of cheap solar concentrators. These are prominent in the SEGs plants of the Mojave Desert in the USA. One such plant is the new *Solargenix* 64MW generation facility in Nevada (Solargenix Operating Services Co., 2006). Thus it would be desirable to tailor the ammonia dissociation process to this existing market of solar concentrators.

Figure 1—2 : An array of LS-2 trough concentrators in California. (Source: Kramer Junction Company.)

Trough concentrators provide much lower concentration ratios than their dish counterparts, and hence are fundamentally limited to lower operating temperatures. In addition, trough concentrators feature a linear focus, rather than a point focus. This leaves a greater area from which to lose heat.

The aim of this project was to investigate heat losses from trough reactors. This would allow the reactor geometry to be optimised for trough concentrators in future investigations. To this end, heat loss experiments were carried out with a short model receiver containing heating elements. This featured the same cross-sectional geometry as the existing receiver for the trough. Data from actual solar dissociation experiments was then used to test and calibrate the heat loss model developed from the small-scale receiver. The final step in the investigation was to compare reaction parameters from a computer simulation to those obtained during solar dissociation experiments.

2. MODELLING RECEIVER HEAT LOSSES

Paitoonsurikarn (2006) and Taumoefolau (2004) had previously studied the heat losses from cylindrical cavity receivers for dish concentrators. Trough cavity receivers, on the other hand, consist of a long rectangular prism, as pictured in Figure 2—1. Therefore, a new investigation of heat losses was necessary, and a small-scale receiver was constructed as per Figure 2—1. Experiments were then carried out to measure the total heat losses. These were especially important for modelling convection losses, as such losses are harder to predict with theory than are conduction or radiation losses. This is because convection problems involve the solution of complex partial differential equations, for which not all of the parameters are known (Holman, 1999). A complementary method to model convective losses would be to use a computational fluid dynamics (CFD) software package, similar to the CFD modelling work performed by Paitoonsurikarn (2006).

Once an empirical relation for the free convection heat loss coefficient had been found, this was compared to that predicted using the free convection correlation developed by Paitoonsurikarn (2006). This comparison was chosen over a comparison with the model developed by Taumoefolau (2004), as Paitoonsurikarn's model was designed to account for differences in the receiver geometry. Due to time constraints of the project, no investigation of forced convection losses was conducted.

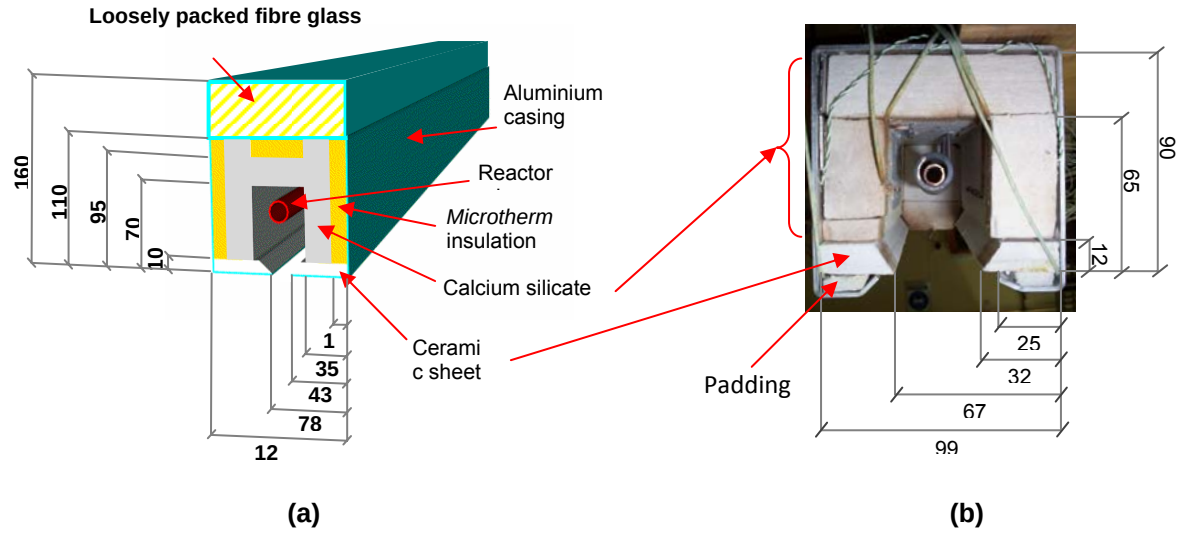

Figure 2—1 : Cross-sections of the full-sized cavity receiver (a), and the short receiver (b). Dimensions are given in millimetres. The full-sized receiver and reactor are 1500mm and 1080mm in length respectively. The short receiver was 200mmin length.

2.1. Heat Loss Apparatus and Procedure

Figure 2—2. Left : The apparatus used to set the angle of inclination for the small-scale receiver, 30 degrees in the photo. Top right : A front view of the cavity and heating elements for the small-scale receiver. Bottom right : The blocked cavity set up used to measure conduction losses.

The total heat losses for the small-scale receiver were measured using the open-cavity arrangement shown in Figure 2—2. The element temperatures were set in 25 degree increments from 200°C to 575°C. The energy used by the elements to maintain their temperature for 15 minutes at steady state was then recorded with a *Powermate* power meter. This procedure was repeated for each angle of inclination, from 0 degrees (horizontal cavity), to 90 degrees (cavity facing down vertically).This gave the total heat losses for each angle of inclination and element temperature, as graphed in **Error! Reference source not found.** and **Error! Reference source not found.**. The losses due solely to

conduction were then measured using a similar procedure, but with a blocked cavity, as pictured in Figure 2—2. These are graphed in Figure 2—3.

2.2. Heat Loss Results

Unlike the conduction losses, radiation losses could not be measured directly. Hence a calculation was performed to determine their contribution to the total heat loss. Taumoefolau (2004) suggested that the free convection losses at an inclination of 90° can be approximated by the convection losses that would occur if the aperture were the lower surface of an isothermal plate. Therefore, we should be able to calculate radiation losses by taking the total heat losses at an inclination of 90°, and subtracting the measured conduction losses, as well as convection losses for the lower surface of a heated plate. These empirically derived radiation losses were compared with those calculated using a radiation network. Both of these radiation calculations carried out for the inclination of 90° should be applicable at any inclination angle, due to the electromagnetic nature of radiation losses.

The results of these radiation calculations are shown by the open triangles and open circles in Figure 2—3. If we add the empirical radiation losses (open triangles) to the conduction losses (open squares), the result is the curve denoted by purple squares. Thus the remainder of the total heat losses for any given inclination gives the free convection heat losses. For example, the bracket overlaid on the graph indicates the convection losses for an inclination of zero degrees and an element temperature of 575°C. These free convection losses are graphed in Figure 2—4 overleaf.

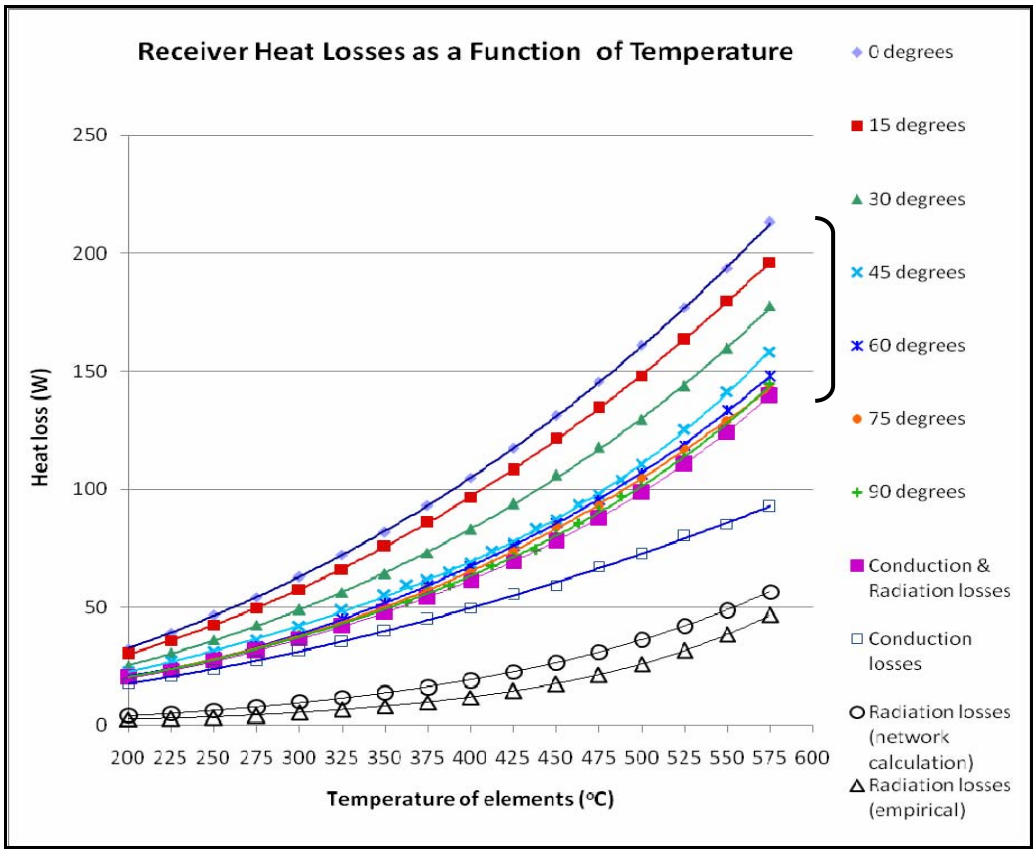

Figure 2—3 : Radiation, conduction and total heat losses for the small-scale receiver. The total heat losses are given by the curves labelled *0 degrees* through to *90 degrees*. Other curves are as labelled.

In general, convection heat loss can be expressed as a function of the temperature difference that drives the loss.

$$q_{convect} = hA(T_f - T_{amb}) \quad \textbf{(2)}$$

Here *h* denotes the free convection heat loss coefficient (in W/m^2.^{o}C), and *A* the surface area. Thus as we have plotted $q_{convect}$ against the temperature difference, we will be able to determine the free convection heat loss coefficient for each inclination angle from the slope of the curves. The values of *h* determined experimentally are given by the blue curve in Figure 2—5.

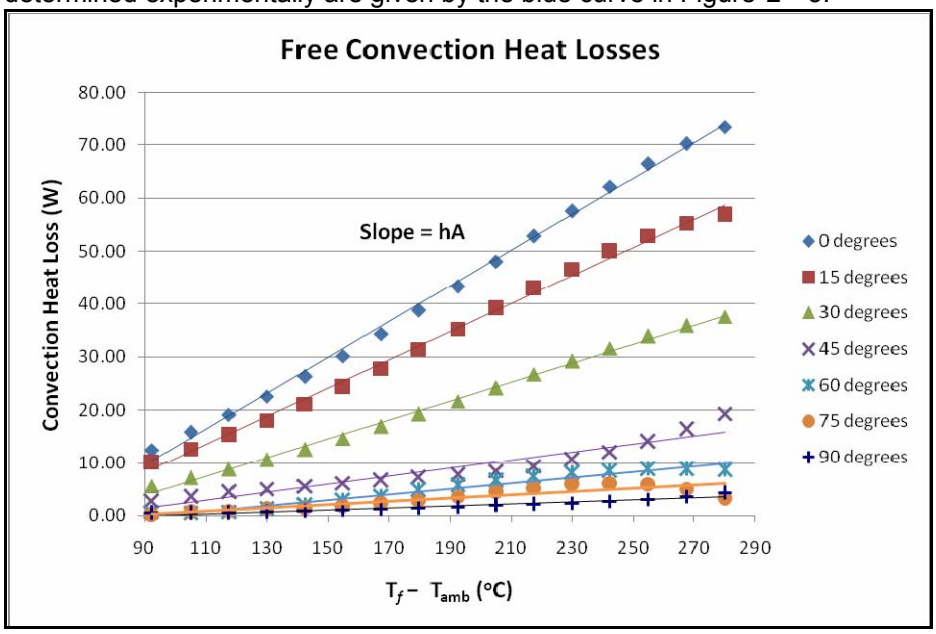

Figure 2—4: Convection heat losses for the small-scale receiver, plotted against the difference between the film temperature, and the ambient temperature. The film temperature (T_f) was taken as the average of the element temperature and the ambient temperature.

2.3. Comparison with the Free Convection Correlation by Paitoonsurikarn

Paitoonsurikarn (2006) developed a correlation to predict the free convection heat losses from cylindrical cavity receivers. This predicted Nusselt numbers of the form:

$$Nu_L = 0.0196 Ra_L^{0.41} Pr^{0.13} \quad \textbf{(3)}$$

where *Ra* and *Pr* are the dimensionless Rayleigh and Prandtl numbers respectively. From this, the convection heat loss coefficient is given by $h = Nuk/L_s$. The length scale L_s is determined as a function of the cavity depth and aperture, as well as the angle of inclination.

Using the dimensions of the small-scale receiver, *h* was calculated from Equation (3), and plotted alongside the free convection heat loss coefficients obtained experimentally. As illustrated in Figure 2—5, there is no agreement between the two sets of heat loss coefficients. This could be due to two factors. Firstly, heat loss from a cylindrical receiver (as modelled by the correlation of Paitoonsurikarn) occurs from a circular aperture, whereas heat loss from a trough receiver occurs from a long rectangular aperture. And secondly, it is suspected that perhaps the cross-sectional dimensions of the trough receiver in question are too small for Paitoonsurikarn's correlation to be valid. This correlation was developed for cavity depths in the order of 50cm, while the trough receiver in question has a depth of only 6.5cm. This is suggested by the very small values of L_s calculated – at zero degrees inclination, for example, L_s was calculated as zero.

However, the experimental results still give an expressions for the free convection heat loss coefficient (*h*) as a function of inclination angle for a trough cavity receiver with the cross sectional dimensions shown in Figure 2—1:

$$h = -8.22\times10^{-7}\theta^4 + 1.60\times10^{-4}\theta^3 - 8.43\times10^{-3}\theta^2 - 5.86\times10^{-2}\theta + 11.5 \quad \textbf{(4)}$$

Here ϑ is the angle of inclination of the receiver in degrees. It should be noted, however, that for trough cavity receivers with heights and widths different to those in Figure 2—1, while the same general trend will apply, the coefficients will be different.

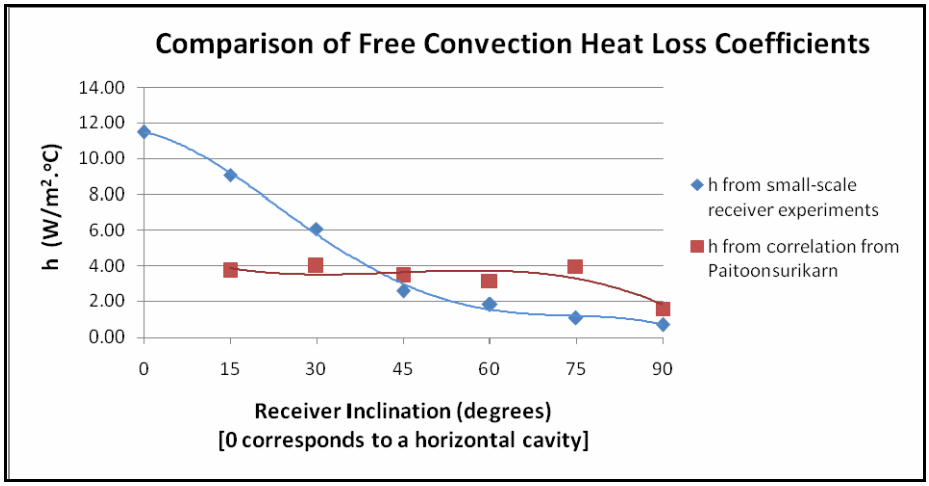

Figure 2—5 : A comparison of the free convection heat loss coefficients determined from the small-scale receiver experiments and those determined using Equation (3).

3. SOLAR DISSOCIATION EXPERIMENTS

In order to test and calibrate the heat loss model developed in Section 2, data from actual solar dissociation experiments was necessary. To this end, solar dissociation experiments were carried out using the trough operated by the *ANU Solar Thermal Group*, as pictured below.

3.1. Solar Dissociation Apparatus & Procedure

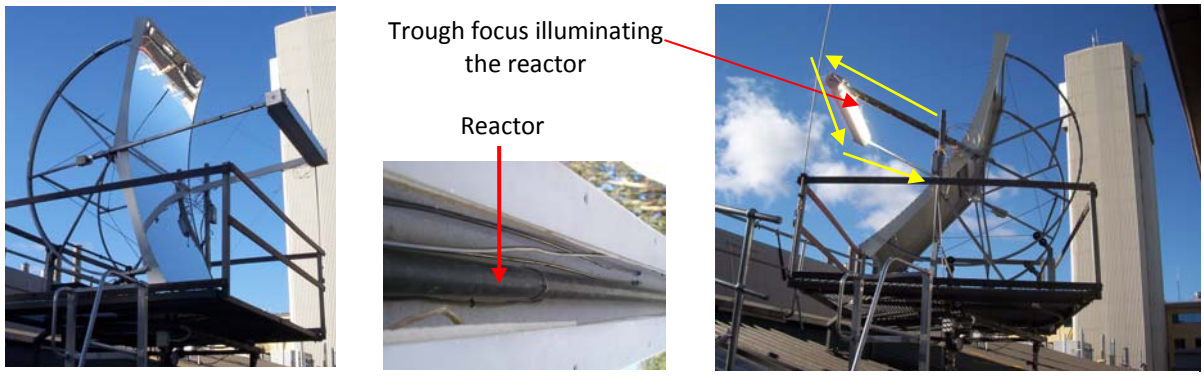

Figure 3—1 : (a) The 2.8m^2 trough concentrator operated by the *ANU Solar Thermal Group*. (b) A close-up of the trough receiver showing the reactor. (c) The trough tracking the sun.

The focal length of the ANU trough is the same as that of the LS-2 troughs, though the mirror chord is only about half that of the LS-2 troughs. The trough is quite short (~1.8 metres in length). Therefore two-axis tracking is employed to ensure that the focus is not "lost" off the end of the receiver. The reactor contains a catalyst bed through which the ammonia is pumped, dissociating as it travels further from the inlet. The flow of ammonia is indicated by the yellow arrows in **Figure 3—1 (c)**. To obtain dissociation data, ammonia was pumped through the reactor at a constant mass flow, with the

receiver "on sun". Once the reactor temperatures had reached steady state (which could take an hour or so), they were left at steady state for 15 to 20 minutes. The mass flow rate was then changed to a new set point. The mass flow rate, wind speed, reactor temperatures, insolation and pressure at the storage vessel were logged throughout the experiment. The solar dissociation experiments performed in this project were all carried out in mid-winter, with a receiver inclination of 35° at solar noon.

3.2. Solar Dissociation Results & Discussion

The mass of ammonia dissociated during each steady state period was determined using the increase in pressure measured at the storage vessel and the ideal gas law. From this, the energy storage rates, system efficiencies and reaction extents for each run were calculated. The reaction extent simply gives the percentage of reactant (ammonia) that has been converted to product (nitrogen and hydrogen gas).

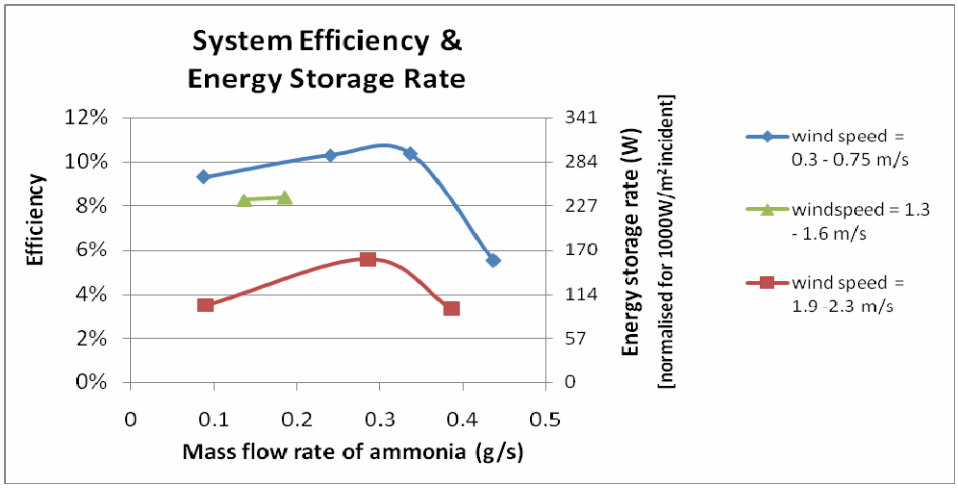

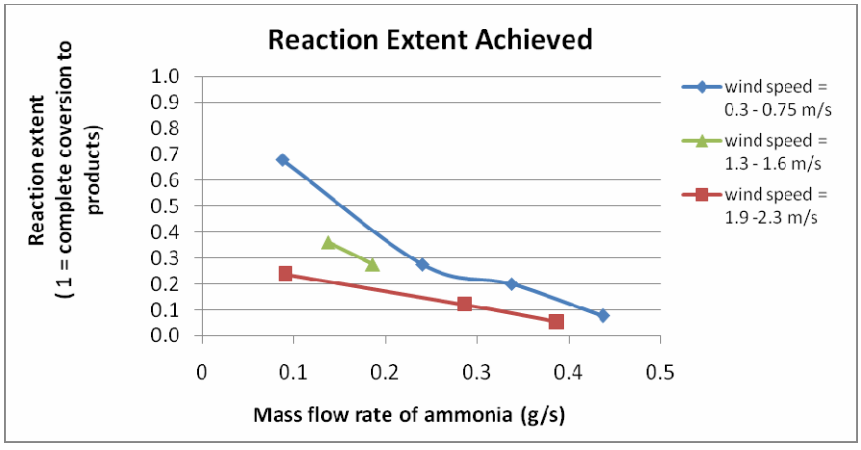

Figure 3—2 : Energy storage rates, system efficiencies and reaction extents for runs at different mass flow rates and wind speeds.

3.2.1. Optimum Flow Rates

First to be analysed is the graph of energy storage rates in **Figure 3—2**. This analysis also applies to the graph of system efficiency, though with a change in units. From the peak in the curves, we can see that the optimum flow rate is around 0.3 g/s, regardless of the wind speed. This may change, however, if the wind speed was to increase significantly. The shape of the curves is also the same regardless of the wind speed. The curves for higher wind speeds are simply translated downwards. This is due to higher forced convection losses at these wind speeds. This effect is quite marked. An increase in wind speed from the range of 0.3 - 0.75m/s to the range 1.9 – 2.3 m/s causes a drop in the energy storage

rate of up to 150W – more than halving the rate. Taking into account that wind speeds of 2 m/s are considered quite low, it is clear that significant optimisation of the reactor and receiver design is necessary in order to minimise losses due to forced convection.

At flow rates below 0.3 g/s, the energy storage rate gradually decreases. Conversely, at flow rates above 0.3 g/s, the energy storage rate decreases rapidly. There is a trade-off, however, between how fast the products exit the reactor, and the degree to which they have been dissociated. This means that even though the reaction extent is highest for low flow rates, because the products are exiting so slowly, the quantity of stored energy exiting the reactor each second will be low. For this reactor, this trade-off between flow rate and final reaction extent is optimal for the flow rate of 0.3 g/s. This is similar to the problem of high flow rates with a solar hot water heater. If the flow rate is too high, a large volume of water can pass through the panel, but all that will be left is a large tank of luke-warm water.

3.2.2. System Efficiency

The maximum efficiency achieved during these runs was 10.3%. This is a far cry from the efficiencies of around 60% obtainable when ammonia dissociation is carried out with a dish concentrator (Lovegreove *et al*. 2004b), and highlights the fact that the current trough reactor and receiver arrangement is not optimised. This was assumed at the outset of the project, and is a driving reason behind studying the heat losses. It is doubtful, however, that efficiencies comparable to that of a dish could ever be achieved with trough reactors, due to the much larger aperture surface area necessary to accommodate the linear focus.

3.2.3. Comparison with Previous Experiments

A series of dissociation experiments had been previously been carried out with the trough in December 2004 and January 2005 by Greg Burgess and Olivier Freitag (Lovegrove et al, 2004b). Unfortunately, these experiments did not involve logging the wind speed, so forced convection losses could not be quantified. Therefore, as accounting for heat losses from the reactor was the primary goal of this project, it was not possible to analyse previously recorded data, except to compare system efficiencies qualitatively. For example, on 20th December 2004, one run was carried out late in the afternoon with a mass flow rate of 0.25 g/s, with a system efficiency of 9.8%. Even though this experiment was carried out in mid-summer, because it was late in the afternoon, the inclination of the receiver would have been close to the inclination of 35^{o} in my experiments. Although nothing is known about forced convection losses for the summer experiment, the free convection losses would have been similar in both circumstances. A comparable experiment that I performed with the same flow rate gave an efficiency of 10.3%. This indicates that the experiments are repeatable, though repetitions of more data points would be necessary to conclude this decisively.

4. HEAT LOSS ACCOUNTING FOR SOLAR DISSOCIATION EXPERIMENTS

Now it was desirable to see if the results from the solar dissociation experiments described in Section 3 could be accounted for using the heat loss models from Section 2. To this end, a *Fortran* simulator for the chemical reaction was used, which accepted a heat flux profile along the reactor as input. The simulator would then predict the temperature profile along the reactor, as well as the reaction extent achieved at each point along the reactor. These predicted temperature profiles and reaction extents would then be compared to those logged during the actual experiments, graphed in Figure 4—1.

The run performed with a mass flow of 0.3g/s and average wind speed of 1.9m/s was chosen for initial investigation with the simulation. This corresponds to the third curve from the bottom in Figure 4—1. To be accurate, it is necessary to calculate the heat flux profile in a iterative process. This is because as the temperature rises or falls along the reactor, so too will the heat losses. A proper implementation of this procedure would involve implementing a loop structure in *Matlab* code (or similar) that repeatedly executed the reactor simulation and calculated new heat flux profiles until the temperatures converged. In the absence of such code, an exponentially decaying flux profile was used as input to the simulation, with the heat flux at the inlet of the reactor calculated using the inlet temperature, as outlined below.

To obtain the heat flux input for the simulation, the radiation and free convection losses were calculated as per the results in Section 2. The insulation for the small-scale receiver from Section 2 was not identical to that in the full-scale receiver. Therefore, conduction losses were calculated using standard 2D conduction formulae and the dimensions from Figure 2—1(a). No study of forced convection losses was carried out during this investigation. Therefore the forced convection loss

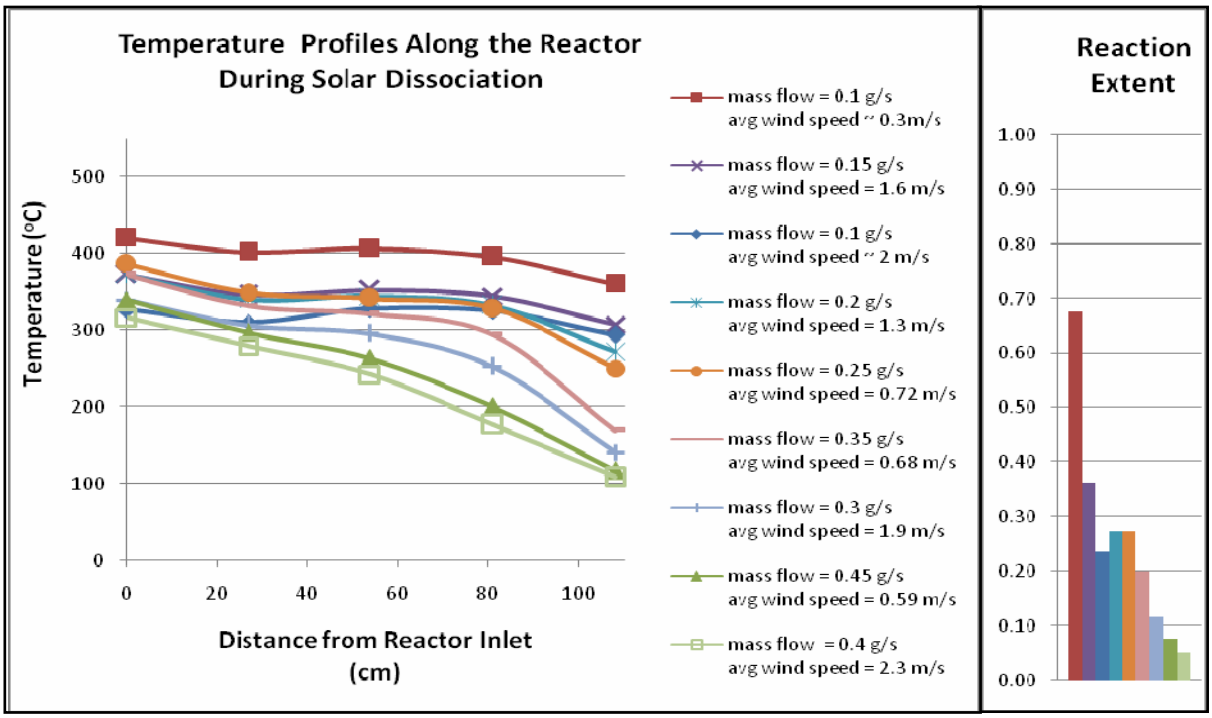

Figure 4—1 : Reactor temperature profiles and reaction extents obtained during solar dissociation experiments.

correlation developed by Taumoefolau (2004) was employed to estimate forced convection losses. This was developed for use with cylindrical cavity receivers, rather than rectangular prism-shaped receivers. However, this gave the best estimate available for forced convection losses. Taumoefolau's correlation gives the Nusselt number for forced convection to be:

$$Nu_L = 0.0033\,(Re)^{0.96}(Pr)^{0.33}h(i) \qquad \textbf{(5)}$$

where *h(i)* accounts for the angle of incidence of the wind. Forced convection heat losses were then calculated in a manner analogous to that used in Section 2.3. Table 4—1 gives a summary of the heat losses calculated, while shows the results of the simulation.

Table 4—1 : Heat loss accounting for a run with a flow rate of 0.3g/s and wind speed of 1.9m/s.

Incident heat flux from focus	2.73 W/cm^2
Conduction losses	0.18 W/cm^2
Radiation losses	0.23 W/cm^2
Free convection losses	0.24 W/cm^2
Forced convection losses	0.83 W/cm^2
Total calculated losses	1.48 W/cm^2
Net heat flux on outer wall of reactor	1.25 W/cm^2

From Figure 4—2, it is clear from the temperature profile that the heat flux profile specified is at least predicting the general decrease in average temperatures along the reactor, though the final temperature is still approximately twice that achieved experimentally. Similarly, the reaction extent predicted for the end of the reactor is twice that achieved in practice.

It should also be noted that the forced convection losses calculated in Table 4—1 are four times any of the other losses calculated. However, it is not known how accurately the correlation developed by Taumoefolau represents forced convection losses from a trough receiver. It could be that the forced convection losses are higher still than those calculated.

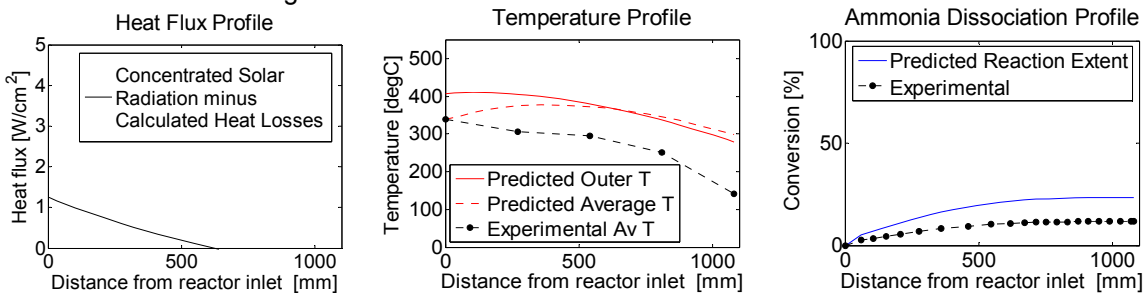

Figure 4—2 : Simulation results for the run with mass flow rate = 0.3g/s and average wind speed = 1.9m/s.

5. CONCLUSIONS & FUTURE RESEARCH

In order to ultimately make the ammonia energy storage system economically viable for trough concentrators, the following points need to be addressed:

- Free convection losses for trough receivers were found not to obey the empirical correlation developed by Paitoonsurikarn (2006). Thus further investigation of free convection losses is necessary to encompass to trough cavities with differing dimensions to those used in this project.
- Further investigation of forced convection losses is necessary. At wind speeds of 2m/s these are believed to account for four times the heat loss of any other mechanism, yet it is not known how accurately the correlation of Taumoefolau predicts losses for trough cavity receivers.
- An iterative procedure for heat loss calculations should be coupled with the existing chemical reaction simulator. This would allow accurate prediction of heat losses and reaction extents along the reactor. The reactor geometry could then be optimised to obtain system efficiencies greater than 10.3%.

6. ACKNOWLEDGEMENTS

Wizard Power Pty Ltd works in conjunction with the ANU Research team to develop the ammonia storage system.

7. REFERENCES

Lovegrove, Keith, Andreas Luzzi, I Soldiani, and Holger Kreetz. “Developing ammonia based thermochemical energy storage for dish power plants.” *Elsevier Science Direct: Solar Energy* (Elsevier Science Direct) 76 (2004a): 331-337.

Lovegrove, Keith, Greg Burgess, Wie Joe, Geoff Major, and Li Ming. *ACT Knowledge fund Proof of Concept: Chemical Storage of Solar Energy With a Trough Concentrator – Final Report.* Canberra: Australian National University, 2004b.

Paitoonsurikarn, Sawat. *Study of a Dissociation Reactor for an Ammonia-Based Solar Thermal System.* A thesis submitted for the degree of Doctor of Philosophy at the Australian National University, 2006.

Taumoefolau, Tu'ifua. *Experimental Investigation of Convection Loss from a Model Solar Concentrator Cavity Receiver.* A thesis submitted for the degree of Master of Philosophy at the Australian National University, 2004.